

Phosphorus-Doped Carbon Nitride Solid: Enhanced Electrical Conductivity and Photocurrent Generation

Yuanjian Zhang,^{*,†,‡} Toshiyuki Mori,[§] Jinhua Ye,^{‡,||} and Markus Antonietti¹

International Center for Young Scientists (ICYS), International Center for Materials Nanoarchitectonics (MANA), Fuel Cell Materials Center, Photocatalytic Materials Center, National Institute for Materials Science (NIMS), 1-1 Namiki, Tsukuba, 305-0044, Japan, and Max Planck Institute of Colloids and Interfaces, Research Campus Golm, D-14424 Potsdam, Germany

Received March 2, 2010; E-mail: ZHANG.Yuanjian@nims.go.jp

Carbon nitrides have attracted worldwide attention, because of the theoretical prediction of their unusual properties.¹ As there are many ways to substitute carbon with nitrogen in graphite, carbon nitrides open various possibilities in constructing scaffolds² with new and exciting properties from mainly C and N. For example, graphitic-C₃N₄ (g-C₃N₄) and its incompletely condensed precursors have shown promising applications in the sustainable energy field as heterogeneous metal-free catalysts for CO₂ reduction.³ This is because they possess a very high thermal and chemical stability and an appealing electronic structure with appropriate band positions and gaps suitable for a variety of relevant chemical reactions.

Very recently, polymeric g-C₃N₄ which is stable to more than 500 °C in air has been exemplified as a promising candidate for solar energy conversion.⁴ However, the efficiency of the proof-of-principle photoelectrochemical cell remains to be improved. The lower efficiencies are partially due to not only poor adaption of the materials interfaces in the cell but also the grain boundary effects that still dominated from our previous report.⁴ Moreover, the optical band gap of pure C₃N₄ is ~2.7 eV, absorbing only blue light up to 450 nm contributing to the primary effect. All these facts are unfavorable for potential applications, especially as organic semiconductors for photovoltaic devices.⁵

Generally, chemical doping is an effective strategy to modify the electronic structures of semiconductors as well as their surface properties, thus improving their performances.⁶ We have reported that a posteriori applied proton doping of g-C₃N₄ not only significantly changed its morphology and surface property but also tuned its electronic structure and enhanced its ionic conductivity.⁷ Localization of electrons by the protons however led to increased band gaps, but the possibility of p-doping by acidification was at least proven. Here we report a “structural doping” strategy, in which the precursors of g-C₃N₄ and a heteroatom source (specifically for phosphorus) were mixed first and then polycondensed together into the final products. This is expected to give a more homogeneous functionalization through the bulk and extended electronic possibilities.

One of the most common ionic liquids, i.e., 1-butyl-3-methylimidazolium hexafluorophosphate (BmimPF₆), was selected as a mild phosphorus source for doping polymeric g-C₃N₄. Ionic liquids are potentially favorable for this process as BmimPF₆ is not volatile and is thermally stable until polycondensation of the matrix monomer Dicyandiamide (DCDA) starts. With a further increase of temperature, PF₆⁻ is expected to react with amine groups to join into the C–N framework. Unwanted elements such as excess hydrocarbons and ammoniumfluoride, with appropriate reaction conditions assumed, can

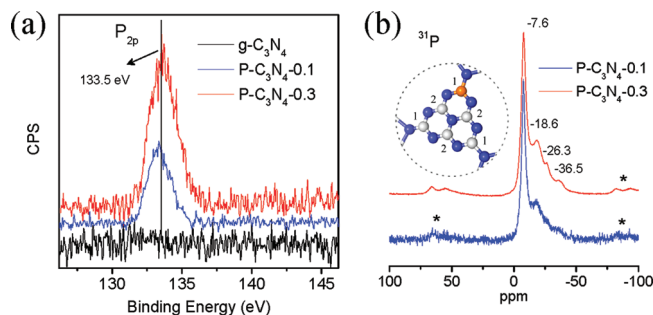


Figure 1. (a) XPS and (b) ³¹P solid-state MAS NMR spectra of P-doped and pristine g-C₃N₄. The asterisks mark spinning sidebands. Inset: the building unit of C₃N₄ with P doping at the corner-carbon site (1, the substitution at bay-carbon site, 2, is not shown). Carbon atoms are gray, nitrogen atoms are blue, and phosphorus atom is orange.

leave the reaction mixture as gaseous species. In this first set of experiments, only doping amounts of BmimPF₆ to DCDA were used, i.e. 10 and 30 wt %, and the resulting products were denoted as P-C₃N₄-0.1 and P-C₃N₄-0.3, respectively.

The structure and texture of the P-doped carbon nitride solids were first evaluated by X-ray diffraction (XRD) and FT-IR. All XRD diffractograms and FT-IR spectra of P-C₃N₄-0.1 and P-C₃N₄-0.3 are very similar to those of pristine polymeric g-C₃N₄, indicating the original graphitic C–N network remained mostly unchanged (Figure S1). The vibrations of the P-related group were hardly observed in doped g-C₃N₄, except for a peak centered at ca. 950 cm⁻¹ (P–N stretching mode), which was presumably because its content was low and its vibration was overlapped by that of C–N. Considering the bigger phosphorus atom and the potentially larger binding lengths in the framework of g-C₃N₄, this is somewhat surprising.

Energy dispersive X-ray microanalysis (EDS) gives direct evidence of a P heteroatom in the doped g-C₃N₄ as well as the degree of doping. For example, the at % of P is ca. 0.6 for P-C₃N₄-0.1, indicating that ca. 30% phosphorus from BmimPF₆ has been introduced into the doped g-C₃N₄ lattice (3.8 at % for P-C₃N₄-0.3, Table S1). The elemental mapping images indicate that P is homogeneously distributed in the whole host of doped g-C₃N₄ solid (Figure S2). Moreover, elemental analysis shows that the C/N ratios of g-C₃N₄ before and after doping are quite similar to the theoretical value for C₃N₄ (0.75). By increasing the initial BmimPF₆ portion, C/N is slightly increased, but the quantity of the final product however becomes smaller, indicating the presence of some side reactions between the “reactive” fragments of BmimPF₆ and carbon nitride precursors toward volatile intermediates; i.e., the reaction is not stoichiometrically balanced.

Further structural details on the incorporation of P into the C/N-scaffold were obtained with X-ray photoelectron spectroscopy (XPS, Figure 1a) measurements. The P_{2p} binding energy (BE) peaks of

[†] ICYS, NIMS.

[‡] MANA, NIMS.

[§] Fuel Cell Materials Center, NIMS.

^{||} Photocatalytic Materials Center, NIMS.

¹ Max Planck Institute of Colloids and Interfaces.

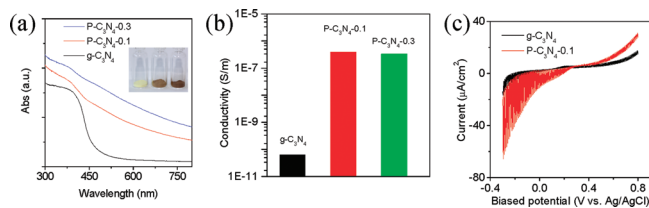


Figure 2. UV-vis spectra (a) and electrical conductivity (b) of P doped and pristine $g\text{-C}_3\text{N}_4$. Inset: photographs for $g\text{-C}_3\text{N}_4$ (left), $\text{P-C}_3\text{N}_4\text{-0.1}$ (middle), and $\text{P-C}_3\text{N}_4\text{-0.3}$ (right). (c) Current-potential curve of P-doped and pristine $g\text{-C}_3\text{N}_4$ photoelectrodes in 0.1 M aqueous KCl under chopped visible light ($\lambda > 420$ nm, 150 W Xe lamp), chopping frequency: ~ 0.5 Hz, scan rate: 10 mV/s.

P-doped $g\text{-C}_3\text{N}_4$ are centered at ca. 133.5 eV, which is typical for a P–N coordination (P–C bonding would be $\sim 1\text{--}2$ eV lower⁸), while that of pristine $g\text{-C}_3\text{N}_4$ naturally only shows negligible contributions. In addition and most relevant, no fluorine could be detected in the final material. Moreover, NMR investigations of doped $g\text{-C}_3\text{N}_4$ on the ³¹P show four well-resolved signals between 0 and -40 ppm, which corresponded to four different positions in the framework structure (Figure 1b). Thus the phosphorus heteratoms most probably replace the corner or bay carbon in the structure forming P–N bonding in the doped C_3N_4 framework, which has four positions, considering neighbor effects to the next layers (ABA stacking).

The nitrophilicity of P is well-known (e.g., P_3N_5 is a very stable species),⁹ and also P–N backbone polymers are useful for materials purposes, so this mode of substitution follows the expectations of a chemist. However the P–N bond length (150–170 pm)^{9b,c} is much longer than that of C–N (135 pm) in carbon nitride,¹⁰ so the incorporation of P heteratoms is expected to compromise a planar structure in doped $g\text{-C}_3\text{N}_4$. Nevertheless, $\text{P-C}_3\text{N}_4$ still retained high stability up to 500 °C in air (Figure S3).

Obviously a final clarification of the exact positioning of P in the structure relies on more detailed experimental characterization. In the present state we can only claim homogeneity of incorporation in the resulting doped carbon nitride via carbon sites, while the characteristic structural properties of polymeric $g\text{-C}_3\text{N}_4$, such as the original graphitic structure, C–N heterocycle units, and C/N composition, were essentially retained.

Doping with a lower percentage of P heteratoms did however remarkably change the electronic structure of $g\text{-C}_3\text{N}_4$, which was anticipated for the potential applications. Photographs of doped and pristine $g\text{-C}_3\text{N}_4$ powders already indicate this influence; i.e., the color turned obviously from yellow to brown (Figure 2a inset). This of course can be quantified by the optical absorption spectra (Figure 2a). It was found that the optical band gap energy is shifted gradually to lower energies for doped $g\text{-C}_3\text{N}_4$ with increasing P content, which indicates again the electronic integration of the P-heteratoms in the lattice of $g\text{-C}_3\text{N}_4$.

Indeed, P-doped $g\text{-C}_3\text{N}_4$ also showed a significant increase in electric conductivity by up to 4 orders of magnitude (Figure 2b), indicating a higher charge-carrier density, also favoring transport in photovoltaic applications. But these conductivities are still numbers gained from pressed powders; that is, the real specific conductivities of the materials are expectedly much higher.

We are not sure if the moderate doping of phosphorus could influence the band gap of carbon nitride as such, but UV-vis absorption at least revealed the introduction of some intermediate states between the valence band and conduction band, which can exchange with the bands as proven by conductivity measurements (see Supporting Information). As expected, the increase in conductivity is not proportional to the phosphorus content as seen by the comparison of $\text{P-C}_3\text{N}_4\text{-0.1}$ and $\text{P-C}_3\text{N}_4\text{-0.3}$. We attribute that to an increasing distortion

of the planar graphitic conduction pathways by the bulky phosphorus; also the bonding angle of P–N in P_3N_5 significantly deviates from 120°.

As one of the most important potential applications of polymeric semiconductors is in the sustainable energy field, Figure 2c shows the photocurrent generation of P-doped $g\text{-C}_3\text{N}_4$. Profiting from more efficient light harvesting (Figure 2a, Figure S4) and the increased electric conductivity (Figure 2b), the photocurrent is remarkably higher than that of pristine $g\text{-C}_3\text{N}_4$, especially when a negative bias potential was applied. The negative photocurrent indicates that holes dominate the charge transport. Moreover, differential pulse voltammetry plots of doped $g\text{-C}_3\text{N}_4$ (DPV, Figure S5) show the reduction peak currents are proportional to the concentration of the dopant. Thus, we can speculate that this is due to the forced planar coordination of the phosphorus, leaving (after oxidation) a partial positive charge on the scaffold carrying the electric current.

In summary, phosphorus was doped into polymeric $g\text{-C}_3\text{N}_4$ by a co-condensation strategy between dicyandiamide and a phosphorus-containing ionic liquid. Due to that the P-concentration was low, the doping well retained most of the structural features of $g\text{-C}_3\text{N}_4$, but electronic features had been seriously altered. This provided not only a much better electric (dark) conductivity up to 4 orders of magnitude but also an improvement in photocurrent generation by a factor of up to 5, which is a significant step toward the photovoltaic applications of polymeric $g\text{-C}_3\text{N}_4$. Yet, methods for preparing such films as cohesive thin layers with oriented domains remain to be found. Besides being active layers in solar cells, such phosphorus-containing scaffolds and materials are also interesting for polymeric batteries as well as for catalysis and as catalytic supports. Work focused in these directions is currently ongoing.

Acknowledgment. We thank Dr. J. Epping (TU Berlin) for help in NMR and Prof. L. Niu (CIAC) for useful discussions. This work was partly supported by World Premier International Research Center (WPI) Initiative on Materials Nanoarchitectonics (MANA), MEXT, Japan, and the Max Planck Society, Germany.

Supporting Information Available: Experimental details, Figures S1–S5, and more discussions. This material is available free of charge via the Internet at <http://pubs.acs.org>.

References

- (1) Liu, A. Y.; Cohen, M. L. *Science* **1989**, *245*, 841–842.
- (2) (a) Komatsu, T. *J. Mater. Chem.* **2001**, *11*, 802–805. (b) Zhang, Z.; Leinenweber, K.; Bauer, M.; Garvie, L. A. J.; McMillan, P. F.; Wolf, G. H. *J. Am. Chem. Soc.* **2001**, *123*, 7788–7796. (c) Vinu, A. *Adv. Funct. Mater.* **2008**, *18*, 816–827. (d) Jurgens, B.; Irran, E.; Senker, J.; Kroll, P.; Muller, H.; Schnick, W. *J. Am. Chem. Soc.* **2003**, *125*, 10288–10300. (e) Lotsch, B. V.; Doblinger, M.; Schnert, J.; Seyfarth, L.; Senker, J.; Oeckler, O.; Schnick, W. *Chem.—Eur. J.* **2007**, *13*, 4969–80. (f) Holst, J. R.; Gillan, E. G. *J. Am. Chem. Soc.* **2008**, *130*, 7373–7379. (g) Gracia, J.; Kroll, P. *J. Mater. Chem.* **2009**, *19*, 3013–3019.
- (3) Goettmann, F.; Thomas, A.; Antonietti, M. *Angew. Chem., Int. Ed.* **2007**, *46*, 2717–2720.
- (4) Zhang, Y.; Antonietti, M. *Chem. Asia J.* **2010**, doi: 10.1002/asia.200900685.
- (5) Bredas, J. L.; Norton, J. E.; Cornil, J.; Coropceanu, V. *Acc. Chem. Res.* **2009**, *42*, 1691–1699.
- (6) (a) MacDiarmid, A. G. *Angew. Chem., Int. Ed.* **2001**, *40*, 2581–2590. (b) Gong, K. P.; Du, F.; Xia, Z. H.; Durstock, M.; Dai, L. M. *Science* **2009**, *323*, 760–764. (c) Wang, D.-W.; Li, F.; Chen, Z.-G.; Lu, G. Q.; Cheng, H.-M. *Mater. Mater.* **2008**, *20*, 7195–7200. (d) Maciel, I. O.; Campos-Delgado, J.; Cruz-Silva, E.; Pimenta, M. A.; Sumpter, B. G.; Meunier, V.; Lopez-Urias, F.; Munoz-Sandoval, E.; Terrones, H.; Terrones, M.; Jorio, A. *Nano Lett.* **2009**, *9*, 2267–72.
- (7) Zhang, Y.; Thomas, A.; Antonietti, M.; Wang, X. *J. Am. Chem. Soc.* **2009**, *131*, 50–51.
- (8) NIST X-ray Photoelectron Spectroscopy Database, <http://srdata.nist.gov/xps/>.
- (9) (a) Gu, H.; Gu, Y.; Li, Z.; Ying, Y.; Qian, Y. *J. Mater. Res.* **2003**, *18*, 2359–2363. (b) Horstmann, S.; Irran, E.; Schnick, W. *Angew. Chem., Int. Ed.* **1997**, *36*, 1873–1875. (c) Landskron, K.; Huppertz, H.; Senker, J.; Schnick, W. *Angew. Chem., Int. Ed.* **2001**, *40*, 2643–2645.
- (10) Lotsch, B. V.; Schnick, W. *Chem.—Eur. J.* **2007**, *13*, 4956–4968.

JA101749Y